



1  
2  
3  
4  
5  
6  
7  
8  
9  
10  
11  
12  
13  
14  
15  
16  
17  
18  
19  
20  
21

## Streamflow estimation at partially gaged sites using multiple dependence conditions via vine copulas

Kuk-Hyun Ahn<sup>1</sup>

---

<sup>1</sup>Assistant Professor, Department of Civil and Environmental Engineering, Kongju National University, Cheon-an, South Korea; *Corresponding author*; e-mail: [ahnkukhyun@gmail.com](mailto:ahnkukhyun@gmail.com)

24



25

26

## ABSTRACT

27

28 Reliable estimates of missing streamflow values are relevant for water resources planning and  
29 management. This study proposes a multiple dependence condition model via vine copulas for  
30 the purpose of estimating streamflow at partially gaged sites. The proposed model is attractive  
31 in modeling the high dimensional joint distribution by building a hierarchy of conditional  
32 bivariate copulas when provided a complex streamflow gage network. The usefulness of the  
33 proposed model is firstly highlighted using a synthetic streamflow scenario. In this analysis,  
34 the bivariate copula model and a variant of the vine copulas are also employed to show the  
35 ability of the multiple dependence structure adopted in the proposed model. Furthermore, the  
36 evaluations are extended to a case study of 54 gages located within the Yadkin-Pee Dee River  
37 Basin, the eastern U. S. Both results inform that the proposed model is better suited for infilling  
38 missing values. After that, the performance of the vine copula is compared with six other  
39 infilling approaches to confirm its applicability. Results demonstrate that the proposed model  
40 produces more reliable streamflow estimates than the other approaches. In particular, when  
41 applied to partially gaged sites with sufficient available data, the proposed model clearly  
42 outperforms the other models. Even though the model is illustrated by a specific case, it can be  
43 extended to other regions with diverse hydro-climatological variables for the objective of  
44 infilling.

45

46 **Keywords: vine copulas, multiple dependence condition model, streamflow estimation**  
47 **and infilling approach**

48



49 **1. Introduction**

50 Hydrological observation records covering long-term periods are instrumental in water  
51 resources planning and management including the design of flood defense systems and  
52 irrigation water management (Aissia et al., 2017; Beguería et al., 2019). However, available  
53 streamflow data is often limited due to several situations like equipment failures, budgetary  
54 cuts, and natural hazards (Kalteh and Hjorth, 2009). Missing data is particularly observed in  
55 remote catchments where equipment failures are repaired only after significant delays  
56 following extreme events, which can be crucial for hydrological frequency analysis. Hence,  
57 hydrologists often rely on simulated sequences to infill missing data in partially gaged  
58 catchments (Booker and Snelder, 2012) by using two primary modeling approaches such as:  
59 (1) process-based models (i.e., estimating streamflow based on a conceptual understanding of  
60 hydrological processes), and (2) transfer-based statistical models (i.e., transferring information  
61 from gaged to ungaged catchments) (Farmer and Vogel, 2016). This paper focuses on the latter,  
62 which estimates historical daily streamflow at inadequately and partially gaged sites by the  
63 means of a statistical relationship.

64

65 Over the past few decades, a variety of statistical models including simple drainage area scaling  
66 (Croley and Hartmann, 1986), spatial interpolation technique (Pugliese et al., 2014), regression  
67 model (Beauchamp et al., 1989) and flow duration curves (FDCs; Hughes and Smakhtin, 1996),  
68 have been developed. In particular, the flow duration curve method has been regarded as one  
69 of the most trustworthy regionalization approaches (Archfield and Vogel, 2010; Boscarello et  
70 al., 2016; Castellarin et al., 2004; Li et al., 2010; Mendicino and Senatore, 2013). If the target  
71 watershed is completely ungaged, FDCs can be established using regression models to



72 regionalize the parameter sets of defined distributions (e.g., Ahn and Palmer, 2016a; Blum et  
73 al., 2017) or to regionalize a set of primary quantiles (Cunderlik and Ouarda, 2006; Schnier  
74 and Cai, 2014; Zaman et al., 2012). On the other hand, if the target watershed is poorly or  
75 partially gaged, FDC models are built using the following four steps: (1) estimating non-  
76 exceedance probability for recorded streamflow from the target watershed of interest; (2)  
77 selecting one or multiple donor watersheds for the target watershed; (3) transferring the time-  
78 series of non-exceedance probability from the donor watershed(s) for missing streamflow  
79 values; and (4) converting corresponding streamflow values back from the transferred non-  
80 exceedance probability. When FDCs are utilized for partially gaged watersheds, how the donor  
81 watersheds are selected (step 2) and how the probabilities are transferred from the donor  
82 watersheds (step 3) play crucial roles in the FDC framework.

83

84 Many studies have developed diverse approaches for steps 2 and 3 in FDC modelling. While  
85 the basic formulation is that non-exceedance probabilities of the target site are transferred by  
86 those at the single donor site, a weighted average of non-exceedance probability from the  
87 selected donor sites has been suggested by Smakhtin (1999) instead. In addition, Farmer (2015)  
88 adopted a kriging model to regionalized daily standard (i.e., z-scored) probabilities based on  
89 non-exceedance probabilities from many donors in a region, using the quantile function of a  
90 standard normal distribution. Although these studies are promising, the joint distribution of  
91 non-exceedance probability between the target and donor watersheds is modeled based on a  
92 Gaussian assumption which cannot properly permit different percentile values such as extremes  
93 that have different spatial dependence structures from donor sites. To circumvent this limitation,  
94 Worland et al. (2019) suggested the copula theory after showing that a unifying framework of  
95 copulas is equivalent to that of FDC (i.e., estimations of the conditional probabilities at the



96 target watershed given known values at the donors).

97

98 Increasing attention has been paid to copulas in the field of hydrology, with applications in  
99 flood frequency analysis, drought risk analysis, and multi-site streamflow simulations (Ahn  
100 and Palmer, 2016b; Ariff et al., 2012; Chen et al., 2015; Daneshkhah et al., 2016; Fu and Butler,  
101 2014). Copulas are efficient mathematical functions that are capable of combining univariate  
102 marginal distribution functions of random variables into their joint cumulative distribution  
103 function and allow representation of diverse dependence structures between these random  
104 variables corresponding to their family members (Sklar, A., 1959). For example, Fu and Butler  
105 (2014) showed that the Gumbel copula performs well in representing multiple flooding  
106 characteristics as compared to the other copulas from the Archimedean family, namely the  
107 Clayton and Frank copulas. To estimate streamflow (i.e., infilling missing data) at poorly and  
108 partially gaged sites, Worland et al. (2019) have developed bivariate copulas with an  
109 Archimedean copula, but limited their application to a single donor. Albeit the limitation, their  
110 bivariate copulas may be acceptable since the higher dimension of copulas is not rich enough  
111 to model all possible mutual dependencies among multisite donors (see Karmakar and  
112 Simonovic, 2009 for details). Hao and Singh (2013) also describe that multivariate copulas are  
113 incapable of modeling multisite data exhibiting complex patterns of dependence.

114

115 However, if the theoretical limitation of a multivariate copula is mitigated, dependency  
116 information from multiple donor sites may allow more reliable predictions of regionalized  
117 streamflow. Vine copulas, also known as pair copulas, offer a far efficient way to construct  
118 higher dimensional dependence (Bedford et al., 2002; Joe, 1997). They have hierarchical



119 structures that sequentially apply bivariate copulas as the building local blocks for constructing  
120 a higher dimensional copula. The high flexibility of vine copulas enables modeling a wide  
121 range of complex data dependencies. In particular, Aas et al. (2009) have popularized two  
122 classes of vine copulas, canonical vines (C-vines) and drawable vines (D-vines) by allowing  
123 diverse pair-copula families such as the bivariate Student-t copula and bivariate Clayton copula.  
124 After the seminal paper, those two vines have been used in many fields including economics  
125 (Arreola Hernandez et al., 2017; Zimmer, 2015), finance (Dissmann et al., 2013; Lu, 2013),  
126 and engineering (Bhatti and Do, 2019; Erhardt et al., 2015; Xu et al., 2017). Similarly, a few  
127 studies have used vine copulas in hydrologic applications with diverse purposes (Daneshkhah  
128 et al., 2016; Liu et al., 2015; Vernieuwe et al., 2015) although they have not been introduced to  
129 infill missing data.

130

131 Based on the usefulness of vine copulas, Kraus and Czado (2017) have developed a promising  
132 algorithm that sequentially fits such a D-vine copula model ( $\mathcal{M}_{\text{Kraus}}$ ). The algorithm adds  
133 covariates to the model with the objective of maximizing a conditional likelihood and stops  
134 adding covariates to the model when none of the remaining covariates can significantly  
135 increase the model's conditional likelihood. While it is promising, one challenge that can arise  
136 but has not been previously discussed is overfitting when covariates are correlated with each  
137 other. In this situation, the model may adopt ineffective covariates and eventually leads to poor  
138 predictions. In particular, for the purpose of infilling, streamflow values at the target site are  
139 often correlated by those of many donors. Although the structure of  $\mathcal{M}_{\text{Kraus}}$  is potentially  
140 favorable to estimate streamflow, modified model procedure is required to determine the most  
141 influential covariates.



142

143 This study forwards two novel contributions to infill missing data in the field of hydrology: (1)  
144 a D-vine copula-based model is introduced to estimate streamflow for poorly and partially  
145 gaged watersheds and (2) the existing model ( $\mathcal{M}_{\text{Kraus}}$ ) is further improved by incorporating a  
146 new procedure to determine the optimal number of donor sites (namely  $\mathcal{M}_{\text{Dvine}}$ ). First,  
147 synthetic data are generated to compare  $\mathcal{M}_{\text{Kraus}}$  and  $\mathcal{M}_{\text{Dvine}}$ . In this analysis, bivariate  
148 copulas (namely  $\mathcal{M}_{\text{Bicop}}$ ) is also employed to demonstrate the usefulness of a high  
149 dimensional joint dependence structure. Afterwards, a real infilling example is utilized to  
150 compare the proposed vine-based model with six other streamflow-transfer models adopted in  
151 literatures.

152

## 153 **2. Methodology**

### 154 *2.1 D-vine copulas*

155 A copula  $C$  is  $k$ -variate cumulative distribution function on  $[0, 1]^k$  with all uniform margins.  
156 The  $C$  can be understood as a function that links the marginal cumulative distributions  
157  $(F_1, \dots, F_k)$  to form a joint distribution  $F$ . The  $C$  associated with joint distribution  $F$  is a  
158 distribution function  $C: [0, 1]^k \rightarrow [0, 1]$  such that, for all streamflow vector  $\mathbf{q} =$   
159  $(q_1, \dots, q_k)^T$ , the  $C$  satisfies:

160

$$161 \quad F(q_1, \dots, q_k) = C(F_1(q_1), \dots, F_k(q_k)) \quad \text{Eq. (1)}$$

162



163 where  $C$  is unique if  $F_1, \dots, F_k$  are continuous.

164 Based on Sklar's theorem (Sklar, A., 1959), a multivariate distribution function is a  
165 composition of a set of marginal distributions; thus, equation (1) can be expressed in terms of  
166 densities,

167

$$168 \quad f(q_1, \dots, q_k) = [\prod_{i=1}^k f_i(q_i)]c(F_1(q_1), \dots, F_k(q_k)) \quad \text{Eq. (2)}$$

169

170 where  $c$  is a  $k$ -dimensional copula density acquired by partial differentiation of the copula  $C$   
171 (i.e.,  $c(F_1(q_1), \dots, F_k(q_k)) := \frac{\partial^k}{\partial_1 \dots \partial_k} C(F_1(q_1), \dots, F_k(q_k))$ ) and  $f_i(\cdot)$  is the marginal density  
172 corresponding to  $F_i(\cdot)$ .

173

174 Following Bedford and Cooke (2001), any copula density  $c(F_1(q_1), \dots, F_k(q_k))$  can be  
175 decomposed into a product of  $k(k-1)/2$  pair copula densities. Aas et al. (2009) adopted this  
176 idea and introduced the copula class of pair copula constructions (PCCs) known as vine copulas.  
177 These copulas are suitable to model various dependency structures. Vine structures established  
178 by  $k(k-1)/2$  pair copulas are arranged in  $k-1$  trees (Brechmann et al., 2013) and can be  
179 categorized as C-vines and D-vines (Liu et al., 2015). This study focuses on D-vines since they  
180 are more widely used in practice (Daneshkhah et al., 2016).

181

182 A D-vine is characterized by the ordering of its variables (see Figure 1). In the first tree, the





183 dependence of the first and second variables, of the second and third, of the third and fourth,  
 184 and so on, is modeled using pair-copulas. In the second tree, conditional dependence of the first  
 185 and third given the second variable (i.e.,  $c_{1,3|2}(F(q_1|q_2), F(q_3|q_2))$ ), the second and fourth  
 186 given the third (i.e.,  $c_{2,4|3}(F(q_2|q_3), F(q_4|q_3))$ ), and so on, is modeled. Similarly, pairwise  
 187 dependencies of two variables are modeled in subsequent trees conditioned on those variables  
 188 which lie between the two variables in the first tree (e.g.,  
 189  $c_{1,5|2,3,4}(F(q_1|q_2, q_3, q_4), F(q_5|q_2, q_3, q_4))$ ). The density of the  $k$ -dimensional D-vine can be  
 190 computed as follows (Aas et al., 2009):

191

$$192 \quad f(q_1, \dots, q_k) = [\prod_{i=1}^k f_i(q_i)] \times$$

$$193 \quad \prod_{j=1}^{k-1} \prod_{i=j+1}^k c_{j,i|j+1:(j+j-1)}(F(q_j|q_{j+1}, \dots, q_{j+j-1}), F(q_i|q_{j+1}, \dots, q_{j+j-1})) \quad \text{Eq. (3)}$$

194

195 where  $c_{j,i|j+1:(j+j-1)}$  indicates the bivariate copula densities.

196 For the five-dimensional D-vine copula as an example in Figure 1, the corresponding vine  
 197 distribution has the joint density as follows:

198

$$199 \quad f(q_1, \dots, q_5) = [\prod_{i=1}^5 f_i(q_i)] c_{12} \cdot c_{23} \cdot c_{34} \cdot c_{45} \cdot c_{13|2} \cdot c_{24|3} \cdot c_{24|3} \cdot c_{35|4} \cdot c_{14|23} \cdot c_{25|34} \cdot$$

$$200 \quad c_{15|234} \quad \text{Eq. (4)}$$

201

202 where  $c_{1,2}(F_1(q_1), F_2(q_2))$  is simply denoted as  $c_{1,2}$ .



203

204 As presented in equation (4), the conditional distribution functions and conditional bivariate  
205 copulas are required in vine copula modeling. The conditional distribution functions  
206  $F(q_j | q_{j+1}, \dots, q_{j+j-1})$ , also known as  $h$ -functions, in equation (4) can be addressed using the  
207 pair-copulas from lower trees by using equation (5). Let  $q_i$  be a conditional value of  
208  $q_{j+1}, \dots, q_{j+j-1}$  and  $\mathbf{v} = \{q_{j+1}, \dots, q_{j+j-1}\} \setminus q_i$  the streamflow vector without  $q_i$  used in the  
209 following recursive relationship (Aas et al., 2009):

210

$$211 \quad h(q_j | \mathbf{v}) := F(q_j | \mathbf{v}) = \frac{\partial C_{ji|\mathbf{v}}(F(q_j | \mathbf{v}), F(q_i | \mathbf{v}))}{\partial F(q_i | \mathbf{v})} \quad \text{Eq. (5)}$$

212

213 where the  $h$ -function is associated with the pair-copula  $C_{ji|\mathbf{v}}$ .

214 More details about D-vines can be found in Bedford et al., (2002) and Czado (2010, 2019).

215

## 216 2.2 Algorithm of D-vine copula-based estimation ( $\mathcal{M}_{\text{Dvine}}$ )

217 Following Kraus and Czado (2017), a two-step estimation procedure is adopted for the  
218 prediction of the streamflow value at the target watershed. The algorithm ( $\mathcal{M}_{\text{Dvine}}$ ) is  
219 developed using two library packages in the R programming language (Bevacqua, 2017;  
220 Schepsmeier et al., 2015).

221



222 Let  $q_k$  be the quantile of streamflow at the target watershed given the streamflow values  
223  $q_1, \dots, q_{k-1}$  from the donor sites. In the first step, the marginal cumulative probabilities  
224  $F_k(q_k)$  and  $F_j(q_j)$ ,  $j = 1, \dots, k - 1$ , are estimated using the semiparametric approach. To be  
225 specific, this study uses the continuous kernel smoothing estimator (Geenens, 2014), which is,  
226 given observed streamflow  $q_i^\zeta$ ,  $\zeta = 1, \dots, \xi$ , at  $i$ th site, defined as  $\hat{F}_i(q_i) = \frac{1}{nh} \sum_{\zeta=1}^{\xi} \Omega\left(\frac{q_i - q_i^\zeta}{h}\right)$ .  
227 Here,  $\Omega(q_i)$  is the “kernel” function with  $\omega(\cdot)$  being a symmetric probability density  
228 function and  $h$  is the parameter controlling the smoothness of the final estimate. In this study,  
229 a Gaussian kernel is used for all  $\omega(\cdot)$ . The estimated cumulative probabilities are then  
230 employed to model the D-vine copula in the second step.

231

232 Next, to easily estimate conditional streamflow values at the target site, the D-vine copula is  
233 fitted with fixed order  $F_k(q_k) - F_{I_1}(q_{I_1}) - F_{I_2}(q_{I_2}) - \dots - F_{I_{k-1}}(q_{I_{k-1}})$ , such that  $F_k(q_k)$  is  
234 the first node in the first tree and the other orders of donors ( $I_1, \dots, I_{k-1}$ ) are decided based  
235 on their correlations to the target site (i.e.,  $F_{I_1}(q_{I_1})$  showing the greatest correlations to  
236  $F_k(q_k)$ ). To build the D-vine copula model, five bivariate copulas (Gaussian, Student-t, Frank,  
237 Gumbel, and Clayton copulas) are considered as potential pair copulas (building blocks) to  
238 represent diverse dependence structures. For example, a Gaussian copula is proper when the  
239 non-exceedance probabilities between two watersheds are associated in the body of their  
240 distribution but are not asymptotically dependent in the both tails. On the other hand, a Gumbel  
241 copula may be appropriate for the situation wherein the non-exceedance probabilities exhibit  
242 tail dependence, where high flows are connected by same rainfall events but low flows are not  
243 correlated (e.g., due to regulation) (Salvadori and De Michele, 2004). Details of the five  
244 bivariate copulas are presented in the Supporting Information. Parameters for the five bivariate



245 copulas are estimated based on Kendall rank-based correlation ( $\rho^T$ ) between sites. The optimal  
246 bivariate copula for each pair copula is determined based on the panelized likelihood function  
247 (i.e., AIC).

248

249 The final number ( $\chi_k$ ) of donor sites is further optimized under a cross-validation approach. In  
250 this approach, 80 % of the regional data are employed for model fitting; the other 20 %, for  
251 testing. Again, this procedure is conducted 5 times, each time using a different set of data for  
252 testing. As a measure for the model's fit, the root mean squared error (RMSE; equation (6))  
253 from observed streamflow at the target site is utilized.

254

$$255 \quad RMSE_{\chi_k} = \sqrt{\frac{1}{\xi} \sum_{\zeta=1}^{\xi} (q_k - \hat{q}_k^{\chi})^2} \quad \text{Eq. (6)}$$

256

257 Finally, conditional streamflow values at the target site can be estimated using the inverse form  
258 of the conditional distribution function (i.e., Eq. 5). To depict the ideas, a trivariate case (i.e.,  
259  $\chi = 2$ ) is considered here. Based on the streamflow values at the donor sites ( $q_2, q_3$ ),  $\hat{q}_1$  can  
260 be obtained using the conditional distribution function  $h(q_1|q_2, q_3)$ . For some fixed  
261 probabilities  $\phi$  (e.g.,  $\phi = 0.1, \dots, 0.9$ ),  $F_1(\hat{q}_1)$  is derived from  $C_{1|2,3}$  using an explicit  
262 function:

263

$$264 \quad C_{1|2,3}^{-1}(\phi|F_2(q_2), F_3(q_3)) = h_{1|2}^{-1}(h_{1|32}^{-1}(\phi|h_{2|1}(F_2(q_2)|F_1(q_1))))|F_1(q_1)) \quad \text{Eq. (7)}$$



265

266 where  $C_{1|2,3}^{-1}$  is the inverse of the copula function given the  $\phi$  quantile curve of the copula  
267 (Liu et al., 2015; Xu and Childs, 2013). Therefore, the  $\phi$ th copula-based conditional quantile  
268 function of streamflow at the target site can be calculated as follows:

269

$$\begin{aligned} 270 \quad q_1(\phi|q_2q_3) &= F_1^{-1}(C_{1|2,3}^{-1}(\phi|F_2(q_2), F_3(q_3))) = \\ 271 \quad F_1^{-1}(h_{1|2}^{-1}(h_{1|32}^{-1}(\phi|h_{2|1}(F_2(q_2)|F_1(q_1))))|F_1(q_1))) \end{aligned} \quad \text{Eq. (8)}$$

272

273 Similarly, for the  $k$ -dimensional case, the  $\phi$ th copula-based conditional quantile function can  
274 be calculated along with streamflow at the  $k-1$  donor sites. To acquire an estimate at the target  
275 site, 1000 samples from uniform distribution over the interval  $[0, 1]$  are generated using Monte  
276 Carlo simulations. In this study, the mean value of these generations is regarded as the best  
277 estimate.

278

### 279 3. Application

280 This study first explores the performance of  $\mathcal{M}_{\text{Dvine}}$  under synthetic example. In this analysis,  
281  $\mathcal{M}_{\text{Bicop}}$  and  $\mathcal{M}_{\text{Kraus}}$  are also employed to show the usefulness of  $\mathcal{M}_{\text{Dvine}}$ . For  $\mathcal{M}_{\text{Bicop}}$ , the  
282 optimal bivariate copula is selected based on the AIC while the five bivariate copulas (Gaussian,  
283 Student-t, Frank, Gumbel, and Clayton copulas) are considered as its potential candidates. A  
284 brief description of two additional models are presented in the supporting information. After



285 that, those three models are used for a real application to 54 stream gages located in a region  
286 of the eastern United States by estimating streamflow in partially gaged locations. Finally,  
287 seven infilling approaches (Table 1) are also utilized and evaluated in a cross-validated  
288 framework to evaluate the performance of the proposed model.

289

### 290 *3.1 Synthetic simulation*

291 Synthetic streamflow data are generated using controlled Monte Carlo experiment to explore  
292 how well the three copula-based models ( $\mathcal{M}_{\text{Bicop}}$ ,  $\mathcal{M}_{\text{Kraus}}$ ,  $\mathcal{M}_{\text{Dvine}}$ ) provide streamflow  
293 predictions at the target site given a complex streamflow data in a pseudo gage network. In this  
294 analysis, a six-dimensional streamflow set  $(q_1^\zeta, q_2^\zeta, q_3^\zeta, q_4^\zeta, q_5^\zeta, q_6^\zeta)$ ,  $\zeta = 1, \dots, \xi =$   
295 2190 (i. e.  $\frac{2190}{365} = 6$  years), is modelled using four bivariate copulas (Gaussian, Student-t,  
296 Flank, and Clayton copulas) and lognormal distributions for margins (see Figure 2).

297

298 The performance of each model is evaluated in a calibration-validation framework. First,  
299 synthetic streamflow data are generated for six-dimensional gage network. Then,  $\varphi$  years of  
300 data are randomly selected to be assumed known at the target gage, and the streamflow for the  
301 remaining  $6-\varphi$  years of data is then estimated as missing values ( $\varphi = 4$  in this analysis). This  
302 process is repeated 20 times to build an ensemble prediction. In particular, this study assumes  
303 the fifth streamflow data (i.e.,  $q_5$ ) to be predicted. In this assessment, two characteristics are  
304 considered to compare the three models: model prediction reliability and uncertainty  
305 quantification skill. Model prediction reliability is tested using the root mean squared error  
306 (RMSE; Eq. 6) and Nash-Sutcliffe efficiency (NSE), which are further described in Section 3.4.



307 Uncertainty quantification skill is judged by the ability of each model to build prediction  
308 intervals (PIs) that correctly bound predictions (see Section 3.4). Here, coverage probabilities,  
309 defined as the proportion of the time that true values occur into these PIs, are employed to show  
310 the usefulness of the proposed model.

311

### 312 *3.2 Application to the Yadkin-Pee Dee River*

313 The Yadkin-Pee Dee River Basin (Figure 3), covering around 18,700 km<sup>2</sup> and one of the largest  
314 river basins in North Carolina and South Carolina (Fisk, 2010), is used as real data to evaluate  
315 infilling ability. The basin flows from the northwestern corner of North Carolina near Blowing  
316 Rock and extends south by southeast, crossing the south-central border of North Carolina into  
317 South Carolina, with slightly more than half of its watershed in North Carolina. Most of the  
318 land covered within the basin is forested or used for agriculture although urban areas of the  
319 basin are expanding.

320

321 Daily streamflow data at 54 gages are gathered throughout the study region from web interface  
322 of the U.S. Geological Survey (USGS) National Water Information System (NWIS) (U.S.  
323 Geological Survey, 2018). The 54 gages are selected based on the following criteria: (1) all  
324 gages are recorded continuously for 15 years of daily streamflow over the period from January  
325 2004 to December 2018, and (2) gages have non-zero daily values for the period in the first  
326 criterion since gages with streamflow values equal to zero require a more flexible modeling  
327 structure. Thus, it is common to model zero flows separately in regionalization studies. Based  
328 on the second criterion, 10 gages are discarded (not shown).



329

### 330 *3.3 Intermodel comparison framework*

331 A set of seven infilling approaches is used in the final assessment (see Table 1): (1)  $\mathcal{M}_{\text{FDC-IDW}}$ ,  
332 (2)  $\mathcal{M}_{\text{IDW-streamflow}}$ , (3)  $\mathcal{M}_{\text{Rho-streamflow}}$ , (4)  $\mathcal{M}_{\text{FDC-highestrho}}$ , (5)  $\mathcal{M}_{\text{DAR-streamflow}}$ , (6)  
333  $\mathcal{M}_{\text{Kriging-streamflow}}$ , and (7)  $\mathcal{M}_{\text{Dvine}}$ . This set of seven models is tested in a cross-validation  
334 framework under two different cases. The two cases consider situations wherein  $\varphi$  have  
335 values of 2 and 8 to represent relatively deficit- and sufficient-records for the target site. Similar  
336 to the comparative assessment to show the usefulness of the proposed copula-based model (see  
337 Section 3.1), each case is repeated 20 times by randomly selecting  $\varphi$  years over the applied  
338 period. The reliability of each model is evaluated using RMSE and NSE metrics over the  
339 validated four-year period randomly selected in the remaining data (i.e., 4 years in  $15-\varphi$  years).

340

### 341 *3.4 Error metrics and error decomposition*

342 As presented in Sections 3.1 and 3.3, the root mean squared error (RMSE; Eq. 6) and Nash-  
343 Sutcliffe efficiency (NSE) are employed to evaluate prediction skills:

344

$$345 \quad NSE = 1 - \frac{\sum_{\zeta=1}^{\xi} (\widehat{q^{\zeta}} - q^{\zeta})^2}{\sum_{\zeta=1}^{\xi} (q^{\zeta} - \overline{q^{\zeta}})^2} \quad \text{Eq. (9)}$$

346

347 The NSE (RMSE) can range from  $-\infty$  to 1 (0 to  $\infty$ ), with higher NSE (lower RMSE) implying  
348 better performance. Both metrics have been commonly used in hydrology analysis (Boyle et





349 al., 2000).

350

351 Following derivations suggested in Gupta et al. (2009), the RMSE can be further decomposed  
352 into three components:

353

$$354 \quad RMSE^2 = MSE = (\hat{\mu} - \mu)^2 + (\hat{\sigma} - \sigma)^2 + 2\sigma\hat{\sigma}(1 - r) \quad \text{Eq. (10)}$$

355

356 where  $\mu$  ( $\hat{\mu}$ ) and  $\sigma$  ( $\hat{\sigma}$ ) represent the average and standard deviation for the observed  
357 (estimated) streamflow, respectively, and  $r$  indicates the estimated correlation coefficient.  
358 The first component  $(\hat{\mu} - \mu)^2$  is a measure of how well the average of the observed  
359 streamflow represents the average of the estimated streamflow; the second component  
360  $(\hat{\sigma} - \sigma)^2$  is a measure of how well the variance of the prediction represents the variance of the  
361 observed streamflow; and the third component  $2\sigma\hat{\sigma}(1 - r)$  is dominated by the correlation  
362 and is defined as the “timing” component (Worland et al., 2019). Using these three defined  
363 components, their absolute contributions are explored in this study.

364

365 In addition, the accuracy of the uncertainty quantification skill is also evaluated for the copula-  
366 based models ( $\mathcal{M}_{\text{Bicop}}$ ,  $\mathcal{M}_{\text{Kraus}}$ ,  $\mathcal{M}_{\text{Dvine}}$ ). To be specific, this study utilizes the PI coverage  
367 probability (PICP), which a common metric for this purpose (He et al., 2017; Niemierko et al.,  
368 2019). It provides the relative number of data points that fall between the defined bounds as  
369 expressed follows:



370

$$371 \quad \text{PICP} = \frac{1}{\xi} \sum_{\zeta=1}^{\xi} \theta_{\zeta} \quad \text{with} \quad \theta_{\zeta} = \begin{cases} 1, & \text{if } q^{\zeta} \in [L^{\zeta}, U^{\zeta}] \\ 0, & \text{else} \end{cases} \quad \text{Eq. (11)}$$

372

373 where  $\theta_{\zeta}$  is the indicator variable if  $q^{\zeta}$  is covered by the  $\zeta$ th PI defined by the lower bound  
374  $L^{\zeta}$  and upper bound  $U^{\zeta}$ . This study examines the prediction accuracy of single quantiles.  
375 Therefore, the lower bound is defined as  $L^{\zeta} = -\infty$  and  $U^{\zeta} = q^{\zeta, \varpi}$  where  $\varpi$  is the  
376 estimated quantile at time  $\zeta$ . Accordingly, the upper bound is not a constant, but is re-assigned.  
377 By subtracting the nominal confidence  $\varpi$  from PICP, the average coverage error (ACE) is  
378 obtained as follows:

379

$$380 \quad \text{ACE} = \text{PICP} - \varpi \quad \text{Eq. (12)}$$

381

382 The metric clearly indicates if the predicted quantile is underestimated ( $\text{ACE} < 0$ ) or  
383 overestimated ( $\text{ACE} > 0$ ) while taking small values around 0 for ideal case.

384

## 385 **4. Results**

### 386 *4.1 Results for synthetic experiment*

387 Prediction results from out-of-samples for the RMSE and NSE metrics are presented for the  
388 three copula-based models ( $\mathcal{M}_{\text{Bicop}}$ ,  $\mathcal{M}_{\text{Kraus}}$ ,  $\mathcal{M}_{\text{Dvine}}$ ) in Table 2. The ACE scores are also



389 described for  $\varpi \in \{0.05, 0.10, 0.50, 0.90, 0.95\}$  in Table 3. When compared to the other  
390 models,  $\mathcal{M}_{\text{Bicop}}$  achieves lower RMSE values in the right tail of the RMSE distribution over  
391 the validation periods, but severely underperforms the majority of the designed experiment,  
392 suggesting this model formulation relying on a single donor leads to poor predictions.  $\mathcal{M}_{\text{Kraus}}$   
393 provides higher RMSE values for all the RMSE distribution, particularly for the right tail of  
394 the RMSE distribution. The model utilizes streamflow data from all donors (i.e., five donor  
395 sites) although the first two gages (Gages 1 and 2) show insignificant associations to the target  
396 site ( $r_{1,5} = 0.11$  and  $r_{2,5} = 0.14$ ).  $\mathcal{M}_{\text{Dvine}}$  unequivocally produces the best predictions.  
397  $\mathcal{M}_{\text{Dvine}}$  adopts streamflow data from two or three donors (Gages 3, 4 and 6) without utilizing  
398 streamflow data from the first two donors when a multiple dependence structure is established  
399 to build an ensemble prediction. It outperforms  $\mathcal{M}_{\text{Bicop}}$  and  $\mathcal{M}_{\text{Kraus}}$  across all validation  
400 periods, besides a few with the worst performance. Even in this case, the maximum RMSE of  
401  $\mathcal{M}_{\text{Dvine}}$  is fairly less than the maximum RMSE of  $\mathcal{M}_{\text{Kraus}}$ .

402

403 In addition, the ACE results present how the three models characterize prediction uncertainty.  
404  $\mathcal{M}_{\text{Dvine}}$  is capable of properly covering the predications across the entire distribution while  
405 slight overestimation occurs for the smallest two quantiles. The remaining upper quantiles also  
406 tend to slightly overestimate the true values but the overestimations are less than the other  
407 models ( $\mathcal{M}_{\text{Bicop}}$ ,  $\mathcal{M}_{\text{Kraus}}$ ). Taken together, the results of the synthetic experiment suggest that  
408  $\mathcal{M}_{\text{Dvine}}$  yields the best predictions among the copula-based models tested.

409

410 *4.2 Performance of the copula-based models in the Yadkin-Pee Dee River*



411 Using the insights developed from the synthetic experiment above, the three copula-based  
412 models are applied to the streamflow data for the Yadkin-Pee Dee River. At first, upper and  
413 lower tail dependences ( $\lambda_{upper}$  and  $\lambda_{lower}$ ) are examined for all two pairs of sites (see Figure  
414 4) using the approach of Schmid and Schmidt (2007). Theoretical background is described in  
415 the Supporting Information (Text S3). Note that in this analysis, the dependences become more  
416 obvious as the values approach unity. Two major insights emerge from this figure. First, many  
417 site-pairs exhibit strong upper tail dependence, suggesting that streamflow variability has a  
418 tendency to be more correlated under high-flow conditions compared to under low-flow  
419 conditions (i.e., asymmetric dependence). The lack of lower-tail dependence may be due to  
420 contributions governing low streamflow such as river regulation. Next, even under high- or  
421 low-flow conditions, there is a wide range of tail dependence across the study basin (i.e.,  
422 heterogeneous dependence). To sum up, a wide range of complex dependencies is observed in  
423 the streamflow data over the study basin. The complex dependences suggest, when streamflow  
424 is estimated from multiple donors, the potential usefulness of considering a multiple  
425 dependence structure, which is one of the main features of vine copulas.

426

427 Figure 5 shows the RMSE and NSE results for the three copula-based models under a “leave-  
428 one-out” cross validation framework. This process is repeated 20 times to build an ensemble  
429 prediction by using test periods randomly defined. For this analysis, five years of data are  
430 selected to be assumed as the observed period at the target gage, and another four years are  
431 randomly selected in the remaining data for the test period. Similar to the results from the  
432 synthetic experiment,  $\mathcal{M}_{Kraus}$  performs poorly in both the RMSE and NSE metrics (median  
433 RMSE = 1.549 and NSE = 0.652). The bivariate copula performs well (median RMSE =



434 1.496), indicating that this approach efficiently leverages available information even though  
435 the information is limited to single donor. Particularly,  $\mathcal{M}_{\text{Bicop}}$  achieves lowest RMSE values  
436 in the upper side of the RMSE box (e.g., third quartile), providing a strong uncertainty  
437 quantification skill for the upper bound. However,  $\mathcal{M}_{\text{Dvine}}$  yields the best median RMSE and  
438 NSE values (= 1.359 and 0.719). Given the heterogeneous dependence conditions (see Figure  
439 4), the high dimensional structures are effective in modeling a complex streamflow gage  
440 network. This feature can substantially improve prediction of target site flows.

441

442 Figure 6a presents the ACE scores described for principal quantiles,  $\omega \in$   
443  $\{0.05, 0.10, 0.20, \dots, 0.90, 0.95\}$ , across all target sites under the cross validation framework.  
444 Figure 6b presents 95% PIs for each model for an example time period (1 May 2018 to 31 July  
445 2018) for one target site (USGS site ID: 02143500). Note that the ACE would ideally take zero  
446 value, regardless of the quantiles. The ACE scores for the three models ( $\mathcal{M}_{\text{Bicop}}$ ,  $\mathcal{M}_{\text{Kraus}}$ ,  
447  $\mathcal{M}_{\text{Dvine}}$ ) range from 0.004 to 0.0007 when considering all the quantiles together. However, the  
448 scores vary depending on the quantiles. For instance, the ACE score for  $\mathcal{M}_{\text{Kraus}}$  is noticeably  
449 positive but is almost zero around the median streamflow, indicating that the model properly  
450 represent uncertainty of the median streamflow.  $\mathcal{M}_{\text{Bicop}}$  and  $\mathcal{M}_{\text{Dvine}}$  result in very similar  
451 ACE scores although  $\mathcal{M}_{\text{Dvine}}$  performs slightly better than  $\mathcal{M}_{\text{Bicop}}$ . The differences in  
452 characterization of prediction uncertainty can be confirmed from a particular target site (Figure  
453 6b).

454

455 Based on the results in Figures 5 and 6,  $\mathcal{M}_{\text{Dvine}}$  has the most reliable overall performance (as



456 judged by model prediction reliability and uncertainty quantification skill) and is selected as  
457 an appropriate copula model to infill missing data in partially gaged. Figure 7 shows an  
458 example application of  $\mathcal{M}_{\text{Dvine}}$  including the optimal donor sites, proper bivariate copulas  
459 and their parameters for one target site (USGS site number #214645022) when the model is  
460 calibrated using the full 15-year record.

461

#### 462 *4.3 Intermodel comparison for streamflow estimation*

463 To assess the predictive skill of the proposed vine copula model, it is compared with six other  
464 statistical models (see Table 1). Figure 8 shows RMSE and NSE for the seven models where  
465 the streamflow values are estimated based on the available data defined by the two different  
466 cases, labeled “deficit record” and “sufficient record” (see Section 3.3). Under all cases, the  
467 vine copula approach outperforms the other infilling approaches. For example, for the  
468 “sufficient record” case, median NSE for  $\mathcal{M}_{\text{Dvine}}$  is 0.673 whereas those for  
469  $\mathcal{M}_{\text{IDW-streamflow}}$  and  $\mathcal{M}_{\text{rho-streamflow}}$  are 0.462 and 0.649, respectively. In this analysis, the  
470 approaches, which are based on streamflow values of the donor sites without utilizing non-  
471 exceedance probability including DAR-streamflow and Kriging-streamflow, yield relatively  
472 increased bias in their predictions. On the other hand, an application of FDC models offers  
473 reliable predictions. For instance, for the “sufficient record” case, median RMSE for  
474  $\mathcal{M}_{\text{FDC-highestrho}}$  is 1.603 compared to that of a direct of using streamflow (e.g., median RMSE  
475 of  $\mathcal{M}_{\text{FDC-streamflow}} = 3.422$  for the sufficient record). Similar interpretation can be found in  
476 the comparison between  $\mathcal{M}_{\text{FDC-IDW}}$  and  $\mathcal{M}_{\text{IDW-streamflow}}$ . The results from these approaches  
477 suggest that utilizing FDC process leads to a reliable estimation, which is a primary structure  
478 in the vine copula. The other noticeable feature is that available data length provides a



479 significant influence on performance of some infilling methods. In particular, this is quite  
480 evident for the vine copula model (median RMSEs: 1.598 and 1.379 for deficit and sufficient  
481 records, respectively).

482

#### 483 *4.4 Prediction error decomposition*

484 The RMSE is decomposed into their components (bias, variance, and timing components) for  
485 both the “deficit record” and “sufficient record” predictions (Figure 9). For the both cases,  
486 prediction errors for all seven models are caused largely by timing components. In particular,  
487 models estimating directly streamflow values (IDW-streamflow, DAR-streamflow, Kriging-  
488 streamflow) produce a somewhat biased component, which increases when a shorter record is  
489 employed in the model. For instance, the timing component for  $\mathcal{M}_{\text{IDW-streamflow}}$  is 4.11 and  
490 3.75 for the “deficit record” and “sufficient record”, respectively. Moreover, timing  
491 components dominate the error metric for all cases. However, the importance of variance  
492 component is increased, especially in three models (FDC-IDW, DAR-streamflow, Kriging-  
493 streamflow). Lastly, the results inform that if the proposed vine copulas approach is adapted,  
494 variance and timing components are better captured, leading to better streamflow estimations,  
495 which is beneficial in the practical applications of water resources management.

496

497 Finally, two predictions are further produced using two additional experiments: (1) the  
498 observed marginal cumulative probabilities (i.e., using all 15 years) and conditional streamflow  
499 values constructed from the partial record (i.e., based on  $\varphi$  years), and (2) the estimated  
500 marginal cumulative probabilities (i.e., based on  $\varphi$  years) and conditional streamflow values



501 constructed from the full record (i.e., all 15 years). Their prediction abilities are evaluated over  
502 the validated four-year period randomly selected in the remaining data. Similar to the previous  
503 analysis, each analysis is tested 20 times. The results from these experiments provide an  
504 inference to better isolate how error components from the two-step procedure (see section 2.2)  
505 influence prediction skill.

506

507 Figure 10 shows the ACE scores from the out-of-sampled predictions using the proposed Dvine  
508 model under the two scenarios. When considering all the quantiles together, the ACE scores  
509 for the two scenarios are 0.003 (scenario #1) and 0.006 (scenario #2) on average under the  
510 “deficit record” prediction. Also, the scores under the “sufficient record” prediction are all  
511 nearly 0.003. Those results of the scores are sufficiently closed to zero, implying that both  
512 predictions are reliable. Yet, compared to the predictions estimated by the cumulative  
513 probabilities estimated by the partial record, and conditional models constructed by full records  
514 (i.e., scenario #2), the ACE scores are achieved better, if the cumulative probabilities are  
515 determined by the full record, except for some of the low and high quantiles. Similar  
516 interpretation can be found in the NSE performance of two scenarios (see insets of Figure 10).  
517 It may suggest that the first procedure (i.e., how to determine the cumulative probabilities for  
518 the target site and its donors) is needed to pay careful attention when  $\mathcal{M}_{\text{Dvine}}$  is utilized.  
519 Nevertheless, the procedure to construct the conditional model in a streamflow gage network  
520 is obviously crucial since the over or under-estimations are observed in many quantiles when  
521 the insufficient sampling is employed in this process.

522

523 **5. Conclusion**





524 This study introduces a multiple dependence conditional model (i.e., vine copulas) to produce  
525 streamflow estimates at partially gaged sites. The model includes a flexible high dimensional  
526 joint dependence structure and conditional bivariate copula simulations. In order to confirm the  
527 usefulness of a multiple dependence structure and the procedure for an appropriate number of  
528 donor sites in the final vine copula model, the bivariate copula model and two types of vine  
529 copulas with their unique procedure to determine the optimal number of donor sites are first  
530 investigated using the generated data. These analyses were further extended in a case study of  
531 the Yadkin-Pee Dee River Basin, the eastern United States by estimating streamflow in partially  
532 gaged locations. In this analysis, six statistical infilling approaches were also employed to  
533 represent applicability of the proposed model.

534

535 Results of the synthetic experiment and application to the Yadkin-Pee Dee River Basin  
536 demonstrate that the propose model has benefits in some aspects. First, a multiple dependence  
537 structure adopted in the proposed model is beneficial. From the massive evaluation experiments,  
538 this study shows that multiple dependence structure clearly outperforms a single dependence  
539 structure although there is the risk of overfitting when too many dependence structures are  
540 employed. Moreover, this study confirms that the proposed multiple dependence structure  
541 model with their optimum number of donor sites produces more reliable streamflow estimation  
542 than other common infilling models. Next, the proposed model allows the development of  
543 confidence intervals to consider prediction uncertainty, which is fairly attractive compared to  
544 other models. For example, Bárdossy and Pegram (2013) argue that confidence intervals  
545 obtained using an ordinary kriging model do not reflect the prediction uncertainty well  
546 particularly on a daily scale. Overall, this study exhibits that a vine copula is potentially an  
547 effective tool to support water resource management planners for objectives like gap-filling or



548 extending missing streamflow records.

549

550 While the results of the proposed model are favorable, there are possible limitations worthy of  
551 further discussion. First, the assessment illustrated in this study focuses on model performance  
552 under cross-validation at partially gaged basins, but additional work is needed to extend the  
553 proposed model to ungaged basins. One possible way is to build a regression based model  
554 with spatial proximity and physical basin characteristics to define associations between the  
555 target and donor sites (e.g., Ahn and Steinschneider, 2019). Second, this study does not  
556 consider potential nonstationarity in FDCs and correlations caused by the influence of  
557 anthropogenic activity and change in land use. Nonstationarity may not be problematic in this  
558 analysis since the assessment is limited to 15 years across the gaging network. However, if  
559 longer records were used, it would be beneficial to consider the potential nonstationarity. This  
560 exploration is left for future work.

561

562 There are several opportunities to improve the model structure. For instance, a vine copula is  
563 able to incorporate more additional conditioning variables. One feasible approach is to add a  
564 time series of climate data (e.g., precipitation) or to decompose a time series of streamflow  
565 from the donor sites into a number of periodic components at different frequency levels through  
566 the wavelet decomposition approach (Kisi and Cimen, 2011).

567

568 Lastly, the results presented here are specific to a study basin used in a case study. The proposed  
569 model has not restricted to other watersheds around the world and its application is further



570 required towards drawing more generalized conclusions. In addition, the model could be used  
571 for the purpose of infilling missing values of other hydrometeorological variables besides  
572 streamflow (e.g., precipitation and soil moisture). For this application, the implementation of a  
573 vine copula with combined discrete and continuous margins (i.e., to account for no rainfall  
574 days) should be explored (e.g., Stoeber et al., 2013).

575

#### 576 **Acknowledgements**

577 This work was supported by the National Research Foundation of Korea (NRF) grant funded  
578 by the Korea government (MSIT) (No. 2019R1C1C1002438). Also, the author would like to  
579 acknowledge Scott Steinschneider for his helpful comments during the development of this  
580 paper.

581

#### 582 **REFERENCES**

583

584 Aas, K., Czado, C., Frigessi, A. and Bakken, H.: Pair-copula constructions of multiple  
585 dependence, *Insur. Math. Econ.*, 44(2), 182–198, 2009.

586 Ahn, K.-H. and Palmer, R.: Regional flood frequency analysis using spatial proximity and basin  
587 characteristics: Quantile regression vs. parameter regression technique, *J. Hydrol.*, 540, 515–  
588 526, doi:<http://dx.doi.org/10.1016/j.jhydrol.2016.06.047>, 2016a.

589 Ahn, K.-H. and Palmer, R. N.: Use of a nonstationary copula to predict future bivariate low  
590 flow frequency in the Connecticut river basin, *Hydrol. Process.*, 30(19), 3518–3532,  
591 doi:[10.1002/hyp.10876](https://doi.org/10.1002/hyp.10876), 2016b.

592 Ahn, K.-H. and Steinschneider, S.: Hierarchical Bayesian Model for Streamflow Estimation at  
593 Ungauged Sites via Spatial Scaling in the Great Lakes Basin, *J. Water Resour. Plan. Manag.*,  
594 145(8), 04019030, 2019.

595 Aissia, M.-A. B., Chebana, F. and Ouarda, T. B.: Multivariate missing data in hydrology–  
596 Review and applications, *Adv. Water Resour.*, 110, 299–309, 2017.

597 Archfield, S. A. and Vogel, R. M.: Map correlation method: Selection of a reference streamgage



- 598 to estimate daily streamflow at ungauged catchments, *Water Resour. Res.*, 46(10), 2010.
- 599 Ariff, N., Jemain, A., Ibrahim, K. and Wan Zin, W.: IDF relationships using bivariate copula  
600 for storm events in Peninsular Malaysia, *J. Hydrol.*, 470, 158–171, 2012.
- 601 Arreola Hernandez, J., Hammoudeh, S., Nguyen, D. K., Al Janabi, M. A. and Reboredo, J. C.:  
602 Global financial crisis and dependence risk analysis of sector portfolios: a vine copula approach,  
603 *Appl. Econ.*, 49(25), 2409–2427, 2017.
- 604 Bárdossy, A. and Pegram, G.: Interpolation of precipitation under topographic influence at  
605 different time scales, *Water Resour. Res.*, 49(8), 4545–4565, 2013.
- 606 Bárdossy, A. and Pegram, G.: Infilling missing precipitation records—A comparison of a new  
607 copula-based method with other techniques, *J. Hydrol.*, 519, 1162–1170, 2014.
- 608 Beauchamp, J., Downing, D. and Railsback, S.: Comparison of regression and time-series  
609 methods for synthesizing missing streamflow records, *JAWRA J. Am. Water Resour. Assoc.*,  
610 25(5), 961–975, 1989.
- 611 Bedford, T. and Cooke, R. M.: Probability density decomposition for conditionally dependent  
612 random variables modeled by vines, *Ann. Math. Artif. Intell.*, 32(1–4), 245–268, 2001.
- 613 Bedford, T., Cooke, R. M. and others: Vines—a new graphical model for dependent random  
614 variables, *Ann. Stat.*, 30(4), 1031–1068, 2002.
- 615 Beguería, S., Tomas-Burguera, M., Serrano-Notivol, R., Peña-Angulo, D., Vicente-Serrano, S.  
616 M. and González-Hidalgo, J.-C.: Gap filling of monthly temperature data and its effect on  
617 climatic variability and trends, *J. Clim.*, 32(22), 7797–7821, 2019.
- 618 Bevacqua, E.: CDVineCopulaConditional: Sampling from Conditional C-and D-Vine Copulas,  
619 R package version 0.1. 0., 2017.
- 620 Bhatti, M. I. and Do, H. Q.: Recent development in copula and its applications to the energy,  
621 forestry and environmental sciences, *Int. J. Hydrog. Energy*, 44(36), 19453–19473, 2019.
- 622 Blum, A. G., Archfield, S. A. and Vogel, R. M.: On the probability distribution of daily  
623 streamflow in the United States, *Hydrol. Earth Syst. Sci.*, 21(6), 3093–3103, 2017.
- 624 Booker, D. and Snelder, T.: Comparing methods for estimating flow duration curves at  
625 ungauged sites, *J. Hydrol.*, 434, 78–94, 2012.
- 626 Boscarello, L., Ravazzani, G., Cislighi, A. and Mancini, M.: Regionalization of flow-duration  
627 curves through catchment classification with streamflow signatures and physiographic–climate  
628 indices, *J. Hydrol. Eng.*, 21(3), 05015027, 2016.
- 629 Boyle, D. P., Gupta, H. V. and Sorooshian, S.: Toward improved calibration of hydrologic  
630 models: Combining the strengths of manual and automatic methods, *Water Resour. Res.*, 36(12),  
631 3663–3674, 2000.
- 632 Brechmann, E. C., Hendrich, K. and Czado, C.: Conditional copula simulation for systemic



- 633 risk stress testing, *Insur. Math. Econ.*, 53(3), 722–732, 2013.
- 634 Castellarin, A., Galeati, G., Brandimarte, L., Montanari, A. and Brath, A.: Regional flow-  
635 duration curves: reliability for ungauged basins, *Adv. Water Resour.*, 27(10), 953–965, 2004.
- 636 Chen, L., Singh, V. P., Guo, S., Zhou, J. and Zhang, J.: Copula-based method for multisite  
637 monthly and daily streamflow simulation, *J. Hydrol.*, 528, 369–384, 2015.
- 638 Croley, T. and Hartmann, H.: NOAA Technical Memorandum ERL GLERL-61: Near-Real-  
639 Time Forecasting of Large-Lake Water Supplies: A User’s Manual, Ann Arbor MI, 1986.
- 640 Cunderlik, J. M. and Ouarda, T. B.: Regional flood-duration–frequency modeling in the  
641 changing environment, *J. Hydrol.*, 318(1), 276–291, 2006.
- 642 Czado, C.: Pair-copula constructions of multivariate copulas, in *Copula theory and its*  
643 *applications*, pp. 93–109, Springer., 2010.
- 644 Czado, C.: *Analyzing Dependent Data with Vine Copulas*, Lect. Notes Stat. Springer, 2019.
- 645 Daneshkhah, A., Remesan, R., Chatrabgoun, O. and Holman, I. P.: Probabilistic modeling of  
646 flood characterizations with parametric and minimum information pair-copula model, *J.*  
647 *Hydrol.*, 540, 469–487, 2016.
- 648 Dissmann, J., Brechmann, E. C., Czado, C. and Kurowicka, D.: Selecting and estimating  
649 regular vine copulae and application to financial returns, *Comput. Stat. Data Anal.*, 59, 52–69,  
650 2013.
- 651 Erhardt, T. M., Czado, C. and Schepsmeier, U.: R-vine models for spatial time series with an  
652 application to daily mean temperature, *Biometrics*, 71(2), 323–332, 2015.
- 653 Farmer, W.: Estimating records of daily streamflow at ungauged locations in the southeast  
654 United States, PhD Dissertation Tufts Univ. MA USA, 2015.
- 655 Farmer, W. H. and Vogel, R. M.: On the deterministic and stochastic use of hydrologic models,  
656 *Water Resour. Res.*, 52(7), 5619–5633, 2016.
- 657 Fisk, J.: *Reproductive Ecology and Habitat Use of the Robust Redhorse in the Pee Dee River,*  
658 *North Carolina and South Carolina.*, 2010.
- 659 Fu, G. and Butler, D.: Copula-based frequency analysis of overflow and flooding in urban  
660 drainage systems, *J. Hydrol.*, 510, 49–58, 2014.
- 661 Geenens, G.: Probit transformation for kernel density estimation on the unit interval, *J. Am.*  
662 *Stat. Assoc.*, 109(505), 346–358, 2014.
- 663 Gupta, H. V., Kling, H., Yilmaz, K. K. and Martinez, G. F.: Decomposition of the mean squared  
664 error and NSE performance criteria: Implications for improving hydrological modelling, *J.*  
665 *Hydrol.*, 377(1), 80–91, 2009.
- 666 Hao, Z. and Singh, V. P.: Modeling multisite streamflow dependence with maximum entropy



- 667 copula, *Water Resour. Res.*, 49(10), 7139–7143, 2013.
- 668 He, Y., Liu, R., Li, H., Wang, S. and Lu, X.: Short-term power load probability density  
669 forecasting method using kernel-based support vector quantile regression and Copula theory,  
670 *Appl. Energy*, 185, 254–266, 2017.
- 671 Hughes, D. and Smakhtin, V.: Daily flow time series patching or extension: a spatial  
672 interpolation approach based on flow duration curves, *Hydrol. Sci. J.*, 41(6), 851–871, 1996.
- 673 Joe, H.: *Multivariate Models and Multivariate Dependence Concepts*, Taylor & Francis. [online]  
674 Available from: <http://books.google.com/books?id=iJbRZL2QzMAC>, 1997.
- 675 Kalteh, A. M. and Hjorth, P.: Imputation of missing values in a precipitation–runoff process  
676 database, *Hydrol. Res.*, 40(4), 420–432, 2009.
- 677 Karmakar, S. and Simonovic, S.: Bivariate flood frequency analysis. Part 2: a copula-based  
678 approach with mixed marginal distributions, *J. Flood Risk Manag.*, 2(1), 32–44, 2009.
- 679 Kisi, O. and Cimen, M.: A wavelet-support vector machine conjunction model for monthly  
680 streamflow forecasting, *J. Hydrol.*, 399(1–2), 132–140, 2011.
- 681 Kraus, D. and Czado, C.: D-vine copula based quantile regression, *Comput. Stat. Data Anal.*,  
682 110, 1–18, 2017.
- 683 Li, M., Shao, Q., Zhang, L. and Chiew, F. H.: A new regionalization approach and its  
684 application to predict flow duration curve in ungauged basins, *J. Hydrol.*, 389(1), 137–145,  
685 2010.
- 686 Liu, Z., Zhou, P., Chen, X. and Guan, Y.: A multivariate conditional model for streamflow  
687 prediction and spatial precipitation refinement, *J. Geophys. Res. Atmospheres*, 120(19), 10–  
688 116, 2015.
- 689 Lu, W.: A high-dimensional vine copula approach to comovement of China’s financial markets,  
690 in 2013 International Conference on Management Science and Engineering 20th Annual  
691 Conference Proceedings, pp. 1538–1543, IEEE., 2013.
- 692 Mendicino, G. and Senatore, A.: Evaluation of parametric and statistical approaches for the  
693 regionalization of flow duration curves in intermittent regimes, *J. Hydrol.*, 480, 19–32, 2013.
- 694 Niemierko, R., Töppel, J. and Tränkler, T.: A D-vine copula quantile regression approach for  
695 the prediction of residential heating energy consumption based on historical data, *Appl. Energy*,  
696 233, 691–708, 2019.
- 697 Pugliese, A., Castellarin, A. and Brath, A.: Geostatistical prediction of flow–duration curves in  
698 an index-flow framework, *Hydrol. Earth Syst. Sci.*, 18(9), 3801–3816, 2014.
- 699 Salvadori, G. and De Michele, C.: Frequency analysis via copulas: Theoretical aspects and  
700 applications to hydrological events, *Water Resour. Res.*, 40(12), 2004.
- 701 Schepsmeier, U., Stoeber, J., Brechmann, E. C., Graeler, B., Nagler, T., Erhardt, T., Almeida,



- 702 C., Min, A., Czado, C., Hofmann, M. and others: Package ‘VineCopula,’ R Package Version,  
703 2(5), 2015.
- 704 Schmid, F. and Schmidt, R.: Multivariate conditional versions of Spearman’s rho and related  
705 measures of tail dependence, *J. Multivar. Anal.*, 98(6), 1123–1140, 2007.
- 706 Schnier, S. and Cai, X.: Prediction of regional streamflow frequency using model tree  
707 ensembles, *J. Hydrol.*, 517, 298–309, 2014.
- 708 Sklar, A.: *Fonctions de Répartition À N Dimensions Et Leurs Marges*, Université Paris 8.  
709 [online] Available from: <http://books.google.com/books?id=nreSmAEACAAJ>, 1959.
- 710 Smakhtin, V. Y.: Generation of natural daily flow time-series in regulated rivers using a non-  
711 linear spatial interpolation technique, *Regul. Rivers Res. Manag. Int. J. Devoted River Res.*  
712 *Manag.*, 15(4), 311–323, 1999.
- 713 Stoeber, J., Joe, H. and Czado, C.: Simplified pair copula constructions—limitations and  
714 extensions, *J. Multivar. Anal.*, 119, 101–118, 2013.
- 715 U.S. Geological Survey: National Water Information System (NWISWeb): U.S. Geological  
716 Survey database, [online] Available from: <http://waterservices.usgs.gov/> (Accessed 1 January  
717 2018), 2018.
- 718 Vernieuwe, H., Vandenbergh, S., De Baets, B. and Verhoest, N.: A continuous rainfall model  
719 based on vine copulas, *Hydrol. Earth Syst. Sci.*, 19(6), 2685–2699, 2015.
- 720 Worland, S. C., Steinschneider, S., Farmer, W., Asquith, W. and Knight, R.: Copula theory as a  
721 generalized framework for flow-duration curve based streamflow estimates in ungaged and  
722 partially gaged catchments, *Water Resour. Res.*, 55(11), 9378–9397, 2019.
- 723 Xu, D., Wei, Q., Elsayed, E. A., Chen, Y. and Kang, R.: Multivariate degradation modeling of  
724 smart electricity meter with multiple performance characteristics via vine copulas, *Qual. Reliab.*  
725 *Eng. Int.*, 33(4), 803–821, 2017.
- 726 Xu, Q. and Childs, T.: Evaluating forecast performances of the quantile autoregression models  
727 in the present global crisis in international equity markets, *Appl. Financ. Econ.*, 23(2), 105–  
728 117, 2013.
- 729 Zaman, M. A., Rahman, A. and Haddad, K.: Regional flood frequency analysis in arid regions:  
730 A case study for Australia, *J. Hydrol.*, 475, 74–83, 2012.
- 731 Zimmer, D. M.: Analyzing comovements in housing prices using vine copulas, *Econ. Inq.*,  
732 53(2), 1156–1169, 2015.

733

734

735

736



737

738 **List of Figures**

- 739 Figure 1 Example of D-vine structures with 5 variables, 4 trees and 10 edges  
740
- 741 Figure 2 Structure of the 6-Dimensional vine model and marginal for the synthetic  
742 simulation.  $LN(\pi, \sigma^2)$  denotes the log normal distribution with its mean ( $\pi$ ) and  
743 variance ( $\sigma^2$ ). The target gage is highlighted.  
744
- 745 Figure 3 Map of the Yadkin-Pee Dee Basin with 54 stream gage stations  
746
- 747 Figure 3 Density of the Akaike Information Criterion (AIC) for the six univariate  
748 distributions applied across sites in the study basin. Mean values for each AIC  
749 density are also presented.  
750
- 751 Figure 4 Pairwise upper and lower tail dependence for watersheds in the Yadkin-Pee Dee  
752 River Basin. The upper triangular matrix shows values for the upper-tail  
753 dependence and the lower triangular matrix presents values for the lower-tail  
754 dependence.  
755
- 756 Figure 5 Model performance for the Yadkin-Pee Dee river under a cross-validation  
757 framework based on RMSE (dark squares) and NSE (light squares).  
758
- 759 Figure 6 (a) Average coverage error from three copula-based models for the Yadkin-Pee  
760 Dee River Basin across exemplarily quantiles, and (b) 95% PIs for three models  
761 for an example period (1 May 2018 to 31 July 2018) for a specific target gauge  
762 (USGS ID: 02143500). Observed streamflow (black solid line) is also presented  
763 in each figure.  
764
- 765 Figure 7 Structure of the Dvine copula applied for a particular target site (USGS site  
766 number 214645022) with the defined bivariate copulas and their parameters.  
767
- 768 Figure 8 Inter-model comparison using cross-validation experiments based on RMSE  
769 (upper) and NSE (lower).  
770
- 771 Figure 9 Three contributions from the decomposed mean squared error (MSE) for the  
772 cross-validation experiment with (a) the deficit record and (b) sufficient record  
773 scenarios.  
774
- 775 Figure 10 Average coverage error of the Dvine model for two scenarios under (a) the  
776 “deficit” and (b) “sufficient” cases.  
777  
778  
779  
780  
781  
782





783

784 **List of Tables**

785

786 Table 1 Seven infilling approaches discussed in the study.

787

788 Table 2 RMSE and NSE results over the validation periods under synthetic experiment for  
789 comparing copula-based model formulations. Best metric values for each quantile  
790 are italicized and bolded.

791

792 Table 3 Results of average coverage error (ACE) over the validation periods under  
793 synthetic experiment for comparing copula-based model formulations. Best  
794 metric values for each quantile are italicized and bolded.

795

796

797

798

799

800

801

802

803

804

805

806

807

808

809

810

811

812

813

814

815

816

817

818

819

820

821

822

823

824

825

826

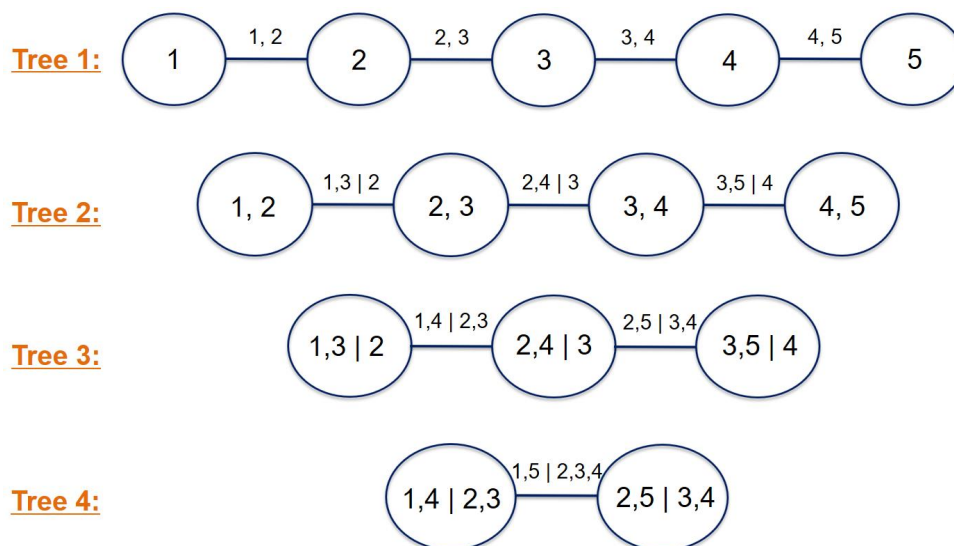
827

828

829



830



831

832 Figure 1 Example of D-vine structures with 5 variables, 4 trees and 10 edges

833

834

835

836

837

838

839

840

841

842

843

844

845

846

847

848

849

850

851

852

853

854

855

856

857

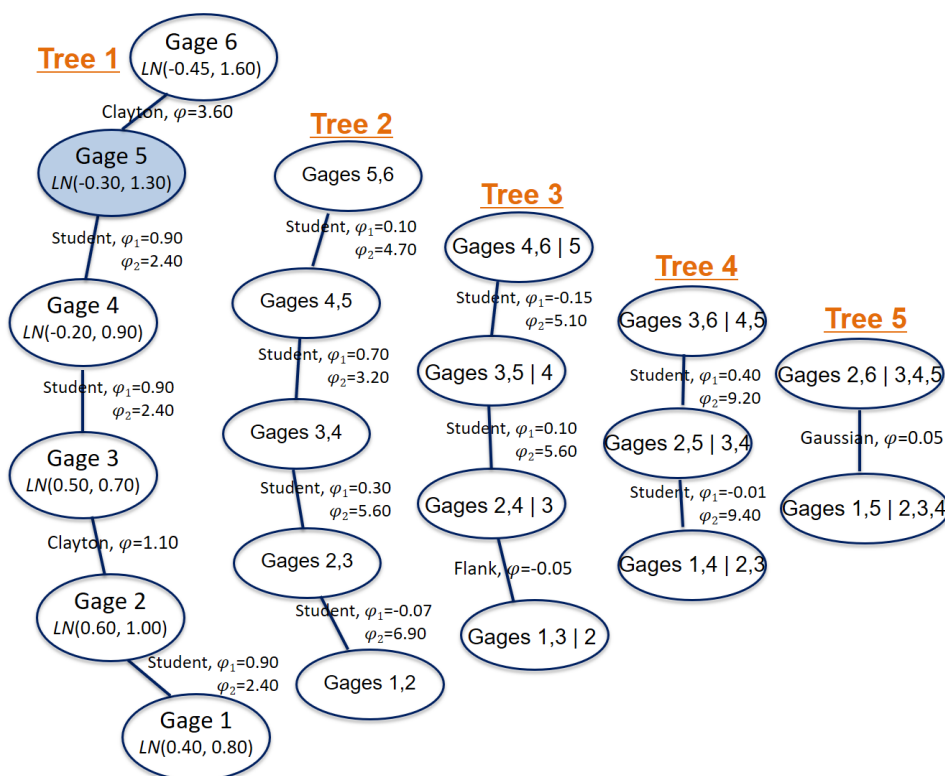
858

859

860



861



862

863

Figure 2 Structure of the 6-Dimensional vine model and marginal for the synthetic simulation.  $LN(\pi, \sigma^2)$  denotes the log normal distribution with its mean ( $\pi$ ) and variance ( $\sigma^2$ ). The target gage is highlighted.

864

865

866

867

868

869

870

871

872

873

874

875

876

877

878

879

880

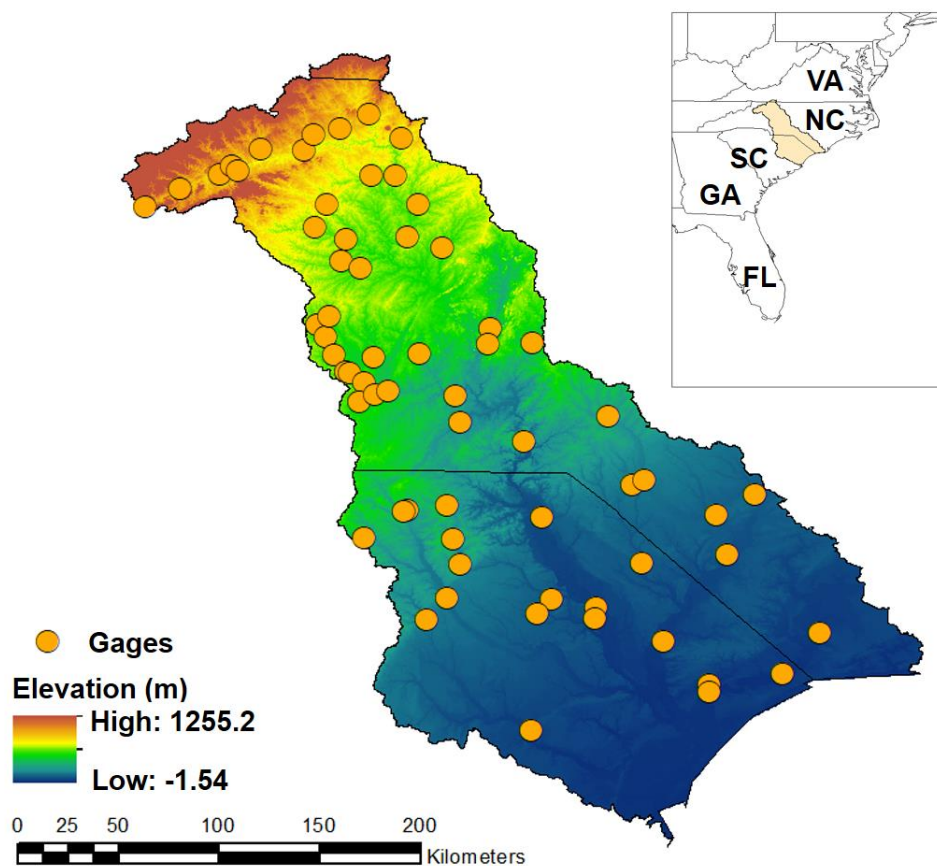
881

882

883



884



885  
886  
887  
888  
889  
890  
891  
892  
893  
894  
895  
896  
897  
898  
899  
900  
901  
902

Figure 3 Map of the Yadkin-Pee Dee Basin with 54 stream gage stations



903

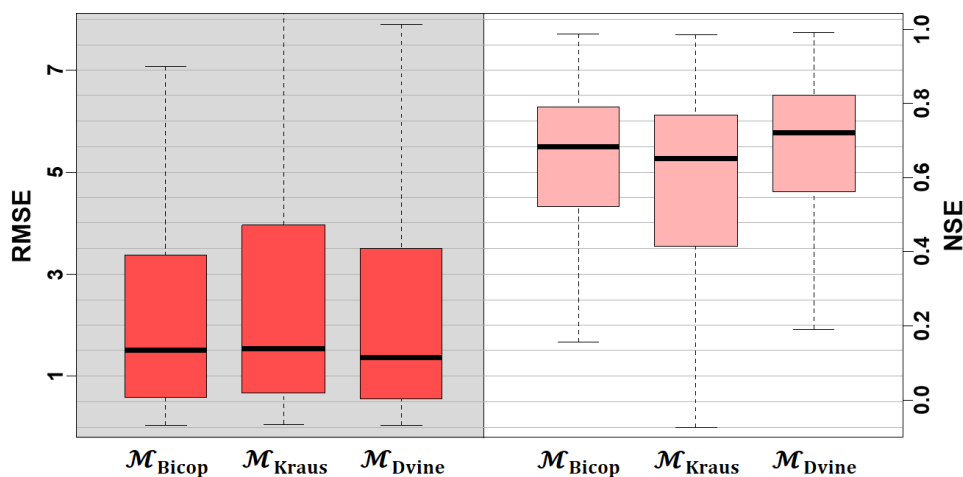


904  
905  
906  
907  
908  
909  
910  
911  
912  
913  
914  
915  
916  
917  
918  
919  
920  
921  
922  
923  
924  
925  
926

Figure 4 Pairwise upper and lower tail dependence for watersheds in the Yadkin-Pee Dee River Basin. The upper triangular matrix shows values for the upper-tail dependence and the lower triangular matrix presents values for the lower-tail dependence.



927



928

929

Figure 5 Model performance for the Yadkin-Pee Dee river under a cross-validation framework based on RMSE (dark squares) and NSE (light squares).

930

931

932

933

934

935

936

937

938

939

940

941

942

943

944

945

946

947

948

949

950

951

952

953

954

955

956

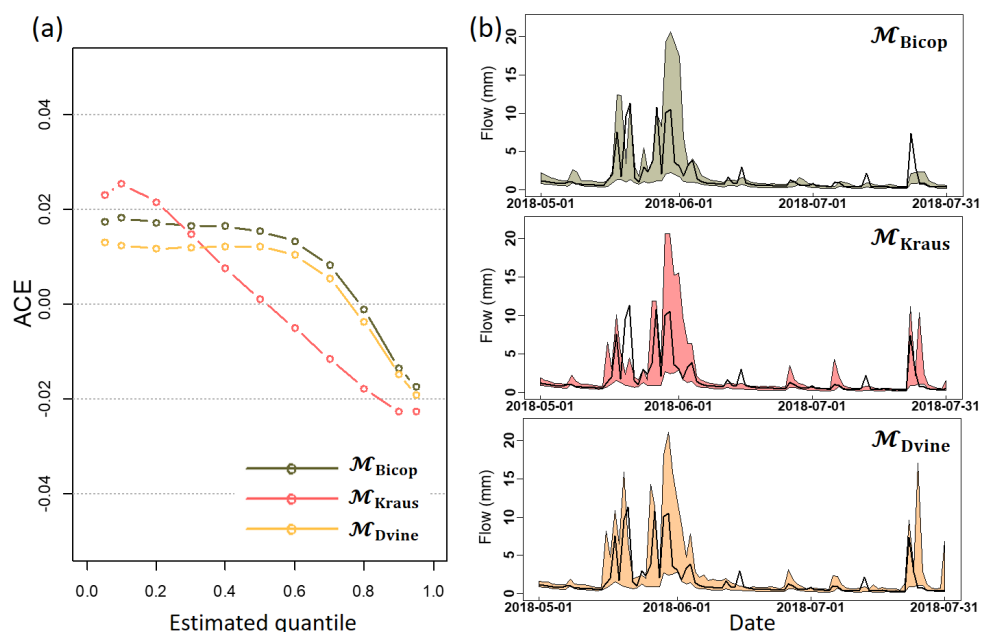
957

958

959



960

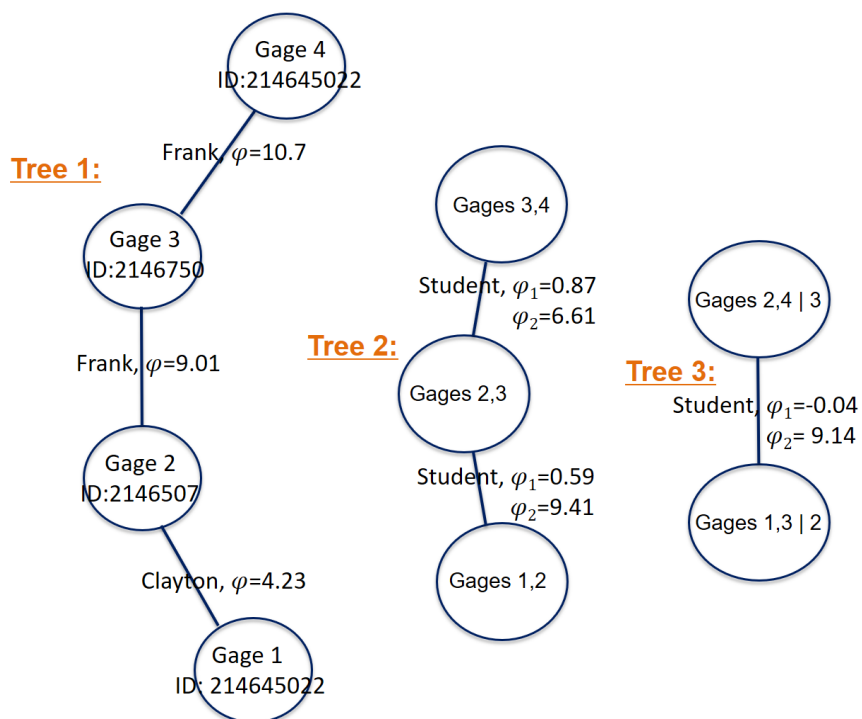


961  
962  
963  
964  
965  
966  
967  
968  
969  
970  
971  
972  
973  
974  
975  
976  
977  
978  
979  
980  
981  
982  
983  
984  
985  
986  
987

Figure 6 (a) Average coverage error from three copula-based models for the Yadkin-Pee Dee River Basin across exemplarily quantiles, and (b) 95% PIs for three models for an example period (1 May 2018 to 31 July 2018) for a specific target gauge (USGS ID: 02143500). Observed streamflow (black solid line) is also presented in each figure.



988



989

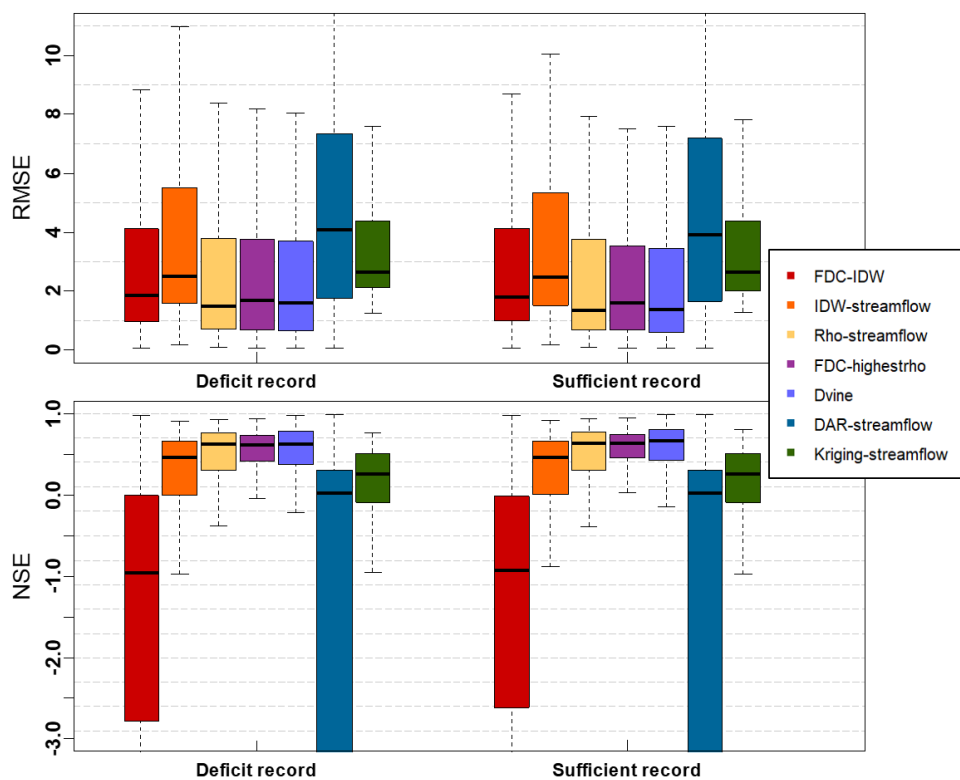
Figure 7 Structure of the Dvine copula applied for a particular target site (USGS site number 214645022) with the defined bivariate copulas and their parameters.

990  
 991  
 992  
 993  
 994  
 995  
 996  
 997  
 998  
 999  
 1000  
 1001  
 1002  
 1003  
 1004  
 1005  
 1006  
 1007  
 1008  
 1009  
 1010  
 1011  
 1012





1013

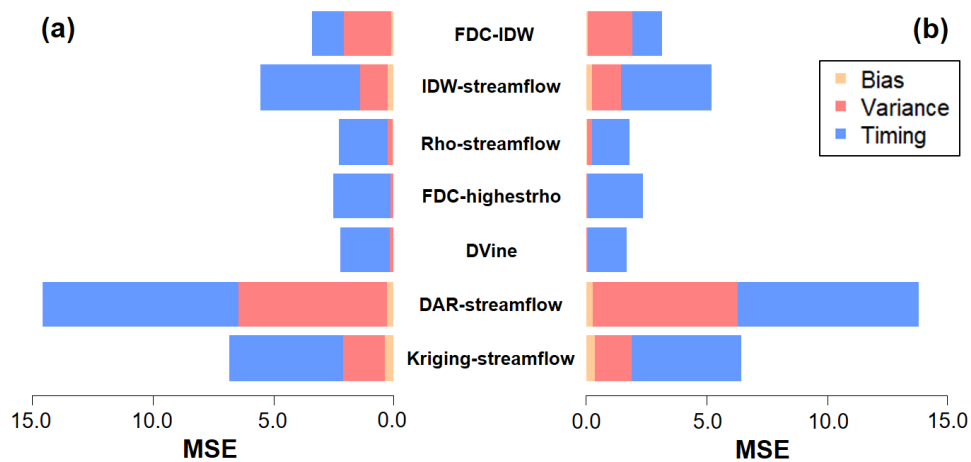


1014  
1015  
1016  
1017  
1018  
1019  
1020  
1021  
1022  
1023  
1024  
1025  
1026  
1027  
1028  
1029  
1030  
1031  
1032  
1033  
1034  
1035

Figure 8 Inter-model comparison using cross-validation experiments based on RMSE (upper) and NSE (lower).



1036



1037

1038

Figure 9 Three contributions from the decomposed mean squared error (MSE) for the cross-validation experiment with (a) the deficit record and (b) sufficient record scenarios.

1039

1040

1041

1042

1043

1044

1045

1046

1047

1048

1049

1050

1051

1052

1053

1054

1055

1056

1057

1058

1059

1060

1061

1062

1063

1064

1065

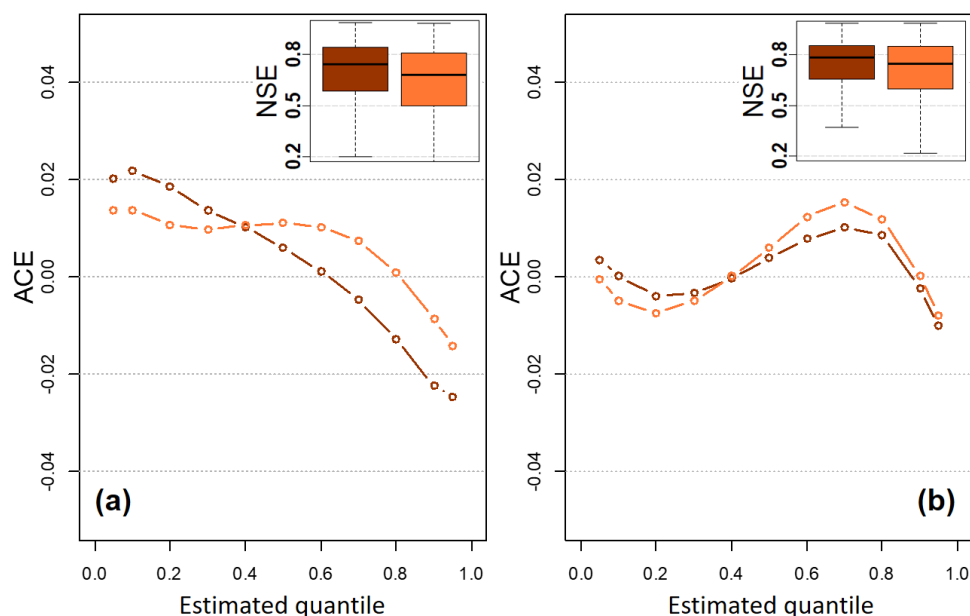
1066

1067

1068



1069



1070

1071

Figure 10 Average coverage error of the Dvine model for two scenarios under (a) the “deficit” and (b) “sufficient” cases. In each case, the dark line represents the scenario by the marginal cumulative probabilities using all years and conditional streamflow values constructed from the partial record. On the other hand, the light line illustrates the scenario by the marginal cumulative probabilities estimated by the partial record and conditional streamflow values constructed from the full record. Inset: NSE performance of the Dvine model for the two scenarios in each case.

1072

1073

1074

1075

1076

1077

1078

1079

1080

1081

1082

1083

1084

1085

1086

1087

1088

1089

1090

1091

1092

1093

1094

1095

1096



1097  
 1098

**Table 1 Seven infilling approaches discussed in the study**

No.	Method	Description
1	FDC-IDW	Inverse distance-weighted estimate of non-exceedance probability from those of all donors.
2	IDW-streamflow	Inverse distance-weighted estimate using streamflow from all donors.
3	Rho-streamflow	Correlation-weighted streamflow estimate from the selected donors for each time step. The optimal number of donors is determined in a cross-validation framework.
4	FDC-highestrho	Estimate non-exceedance probability from the gage with the highest correlation.
5	DAR-streamflow	Drainage-area (DA) ratio for streamflow using the DA from the nearest neighbor gage.
6	Kriging-streamflow	Geostatistical interpolation method to estimate streamflow from all donors for each time step.
7	DVine	Vine copula-based estimate from the selected donors

1099  
 1100  
 1101  
 1102  
 1103  
 1104  
 1105  
 1106  
 1107  
 1108  
 1109  
 1110  
 1111  
 1112  
 1113  
 1114  
 1115  
 1116  
 1117  
 1118  
 1119  
 1120  
 1121



1122  
 1123  
 1124  
 1125

Table 2 RMSE and NSE results over the validation periods under synthetic experiment for comparing copula-based model formulations. Best metric values for each quantile are italicized and bolded.

Metric	Model formulation	Min	First quantile	Median	Third quantile	Max
Root mean squared error (RMSE)	$\mathcal{M}_{\text{Bicop}}$	0.912	1.119	1.258	1.363	<b>3.353</b>
	$\mathcal{M}_{\text{Kraus}}$	0.990	1.140	1.386	1.660	4.273
	$\mathcal{M}_{\text{Dvine}}$	<i><b>0.895</b></i>	<i><b>1.046</b></i>	<i><b>1.112</b></i>	<i><b>1.391</b></i>	4.119
Nash-Sutcliffe efficiency (NSE)	$\mathcal{M}_{\text{Bicop}}$	<i><b>0.464</b></i>	0.779	0.826	0.856	0.902
	$\mathcal{M}_{\text{Kraus}}$	0.198	0.724	0.782	0.825	0.885
	$\mathcal{M}_{\text{Dvine}}$	0.248	<i><b>0.805</b></i>	<i><b>0.838</b></i>	<i><b>0.869</b></i>	<i><b>0.905</b></i>

1126  
 1127  
 1128  
 1129  
 1130  
 1131  
 1132  
 1133  
 1134  
 1135  
 1136  
 1137  
 1138  
 1139  
 1140  
 1141  
 1142  
 1143  
 1144  
 1145  
 1146  
 1147  
 1148  
 1149  
 1150



1151  
1152  
1153  
1154

Table 3 Results of average coverage error (ACE) over the validation periods under synthetic experiment for comparing copula-based model formulations. Best metric values for each quantile are italicized and bolded.

Model formulation	Estimated quantile ( $\varpi$ )				
	0.05	0.10	0.50	0.90	0.95
$\mathcal{M}_{\text{Bicop}}$	0.027	0.063	0.079	0.014	0.002
$\mathcal{M}_{\text{Kraus}}$	<i><b>0.003</b></i>	<i><b>0.011</b></i>	0.055	0.024	0.001
$\mathcal{M}_{\text{Dvine}}$	0.029	0.048	<i><b>0.042</b></i>	<i><b>0.001</b></i>	<i><b>0.000</b></i>

1155  
1156  
1157  
1158  
1159  
1160  
1161  
1162  
1163